Thermodynamics of the Redox Equilibria and the Site Preference in $(Fe_{1-y}Al_y)_{3-\delta}O_4$

Akio NAKAMURA,** Shigeru YAMAUCHI,* Kazuo FUEKI, and Takashi MUKAIBO

Department of Industrial Chemistry, Faculty of Engineering, The University of Tokyo, Hongo, Bunkyo-ku, Tokyo 113

(Received May 18, 1978)

In order to elucidate the defect model in the spinel ferrites, the nonstoichiometry in magnetite and its solid solutions, $(Fe_{1-y}Al_y)_{3-\delta}O_4$, ($y$=0.0, 0.25, 0.33), was determined at temperatures between 1300 and 1550 °C. The redox equilibria between Fe^{2+} and Fe^{3+} and the site preference of Fe^{2+}, Fe^{3+}, and Al^{3+} ions and cation vacancies were investigated and sixteen kinds of models were examined. The "best" model was chosen using the criteria that the dependence of the equilibrium constant on δ and y should be as small as possible. In the selected model, Fe^{2+} ions on B-sites are regarded as electron donors in a narrow 3-d band formed by Fe ions in B-sites. The following expression for the defect equilibrium was found:

$$\frac{2}{3(1-y)}Fe_A^{2+} + \frac{2(2-3y)}{3(1-y)}e_B^- + \frac{1}{2}O_2(g) \rightleftharpoons \frac{2}{3(1-y)}Fe_A^{3+} + \frac{1}{4}V_A + \frac{1}{2}V_B + O_L^{2-}.$$

The thermodynamic properties of the Fe–O system have been studied in relation to the metallurgy and corrosion of steels. Among the oxides of iron, magnetite (Fe_3O_4) has a wide nonstoichiometric range; this attracted much attention in the field of solid state chemistry.[1-3] Magnetite is also regarded as a model compound of spinel-type ferrites, which are industrially important as magnetic oxide materials.

Electrical and magnetic properties of ferrites are largely affected by the charge and distribution of cations and lattice defects, which can be controlled during fabrication processes. Therefore, information about lattice defects in magnetite and ferrites is necessary for the production of ferrites with desired properties.

Magnetite and its solid solutions with $FeAl_2O_4$ have a wide nonstoichiometric composition with cation deficiency at high oxygen pressures.[4] Al^{3+} ions are stable in the spinel structure, so the charge distribution among cations in the spinel ferrite is simpler than in the other ferrites, such as manganese or copper ferrites.

The purpose of this paper is to determine the nonstoichiometry of spinel-type solid solutions of Fe_3O_4 and $FeAl_2O_4$, and to interpret the result on the basis of statistical thermodynamics.

Experimental

Materials. Magnetite was prepared by heating the cold-pressed hematite of 99.99% purity at 1500 °C in air. Solid solutions $(Fe_{1-y}Al_y)_3O_4$ (y=0.25 and 0.33) were formed by heating the cold-pressed powder mixtures of 99.99% pure hematite and alumina in a platinum crucible at 1500 °C in air for 12 h. The X-ray powder diffraction study revealed that the resulting materials were spinel-type solid solutions in a single phase. The weight increase observed when the ferrite specimens were oxidized into alumina and hematite coincided with the values calculated from the composition, within experimental error. The compacts were crushed to grains, 1—2 mm in diameter, and used as samples for the nonstoichiometric measurement.

Measurement of Nonstoichiometry. The apparatus for thermogravimetric measurement has been described elsewhere.[5] About 1 g of crushed oxide sample was placed in a platinum basket suspended from the balance to the furnace heated by a silicon carbide tubular heater. The temperature of the furnace was controlled within ±0.5 °C and the partial pressure of oxygen was controlled within 1—10^{-4} atm by mixing purified oxygen and argon gases.

For the determination of δ-values in $(Fe_{1-y}Al_y)_{3-\delta}O_4$, it was assumed that δ is zero at the phase boundary between wüstite and the ferrites.[5] Such a condition was realized by adjusting the ratio of CO to CO_2 in CO–CO_2 gas mixtures. The nonstoichiometry δ was calculated from the difference in weight.

Corrections for bouyancy, thermomolecular force, and evaporation of platinum were made, based on the results of preliminary experiments.

Results

Nonstoichiometric data of $(Fe_{1-y}Al_y)_{3-\delta}O_4$ (y=0.25, 0.33) obtained in this research are shown in Figs. 1 and 2 as the isothermal curves of log δ *versus* log P_{O_2}. Nonstoichiometric data of magnetite have already been reported,[5] so they are not presented here again. At a constant oxygen partial pressure, the nonstoichiometry decreased with the increase in temperature. The same tendency was observed for Fe_3O_4. The value of δ increased with the increase in aluminum content at an oxygen partial pressure. The slope $(\partial \ln\delta/\partial \ln P_{O_2})$ seems

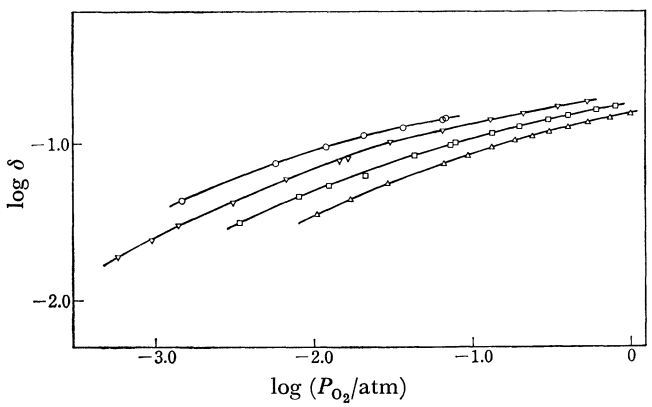

Fig. 1. Nonstoichiometric Data of $(Fe_{0.75}Al_{0.25})_{3-\delta}O_4$.
○: 1350 °C, ▽: 1400 °C, □: 1450 °C, △: 1500 °C.

** Present address: Center for Solid State Science, Arizona State University, Tempe, Arizona 85281, U. S. A.

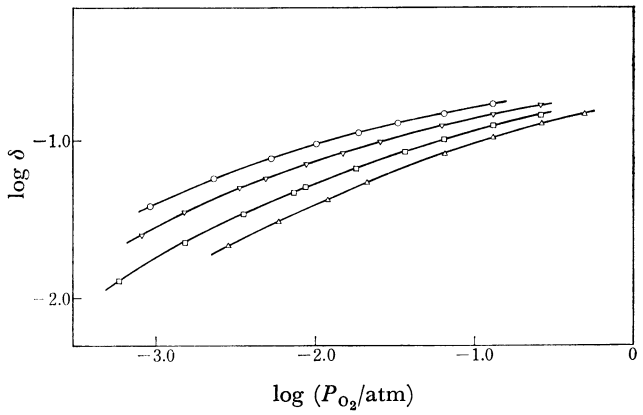

Fig. 2. Nonstoichiometric Data of $(Fe_{0.67}Al_{0.33})_{3-\delta}O_4$.
○: 1400 °C, ▽: 1450 °C, □: 1500 °C, △: 1550 °C.

to decrease slightly with the increase in aluminium content. Thus the same defect model as was suggested for magnetite can perhaps interpret the nonstoichiometry of these solid solutions.

Defect Model

Nonstoichiometry. In the spinel structure, the anion sublattice forms the fcc lattice; thirty two oxide ions are contained in an unit cell. The unit cell also has sixty four tetrahedral cation sites (A-sites) and thirty two octahedral cation sites (B-sites). These cation sites are not completely occupied: only eight A-sites and sixteen B-sites are occupied.[6]

Magnetite is a metal-deficient type oxide. According to Roiter,[4] $Fe_{3-\delta}O_4$ and $FeAl_2O_4$ form a solid solution, which would be a metal-deficit type oxide, in analogy with magnetite. Effective negative charges created by cation vacancy formation are compensated by the conversion of Fe^{2+} ions into Fe^{3+} by the reaction

$$2Fe^{2+} + \frac{1}{2}O_2(g) \longrightarrow 2Fe^{3+} + \frac{3}{4}V_C + O_L^{2-}, \quad (1)$$

where V_C denotes a vacancy on a cation lattice site (A site or B site) and O_L^{2-} denotes an oxide ion on an anion sublattice site.

The mass action law for equilibrium (1) is given by

$$K_1 = \frac{[Fe^{3+}]^2[V_C]^{3/4}}{[Fe^{2+}]^2 P_{O_2}{}^{1/2}}. \quad (2)$$

Equation 2 implies that δ is proportional to $P_{O_2}{}^{2/3}$ as δ is proportional to V_C. The nonstoichiometric data reported so far[1-3] indicate the 2/3 power dependence on P_{O_2} in a small δ range. However, the exponent of P_{O_2} decreases with the increase in δ and reaches 0.33 for magnetite and 0.25 for spinel ferrites. Although Eq. 1 can interpret the nonstoichiometry in magnetite and spinel ferrites qualitatively, internal equilibria and site preference of cations and vacancies have to be taken into account to establish the defect equilibria in spinel ferrite. Thus the analysis was made considering the distribution of cations on A and B sublattices.

Site Preference and Random Distribution of Cations. As mentioned above, the solid solutions have two kinds of cation sites, A-sites and B-sites, on which Fe^{2+}, Fe^{3+}, Al^{3+}, and V_C are distributed. The numbers of Fe^{2+}, Al^{3+}, and V_C on the sublattice are regarded as independent variables. As a pliausble approximation, it can be assumed that the above cations and cation vacancies are distributed either preferentially on A-sites or B-sites or randomly on both sites. The combination of these three kinds of cations and vacancy and the three ways of distribution yields $27(=3^3)$ defect models. Investigations reported so far have elucidated the site preference of each kind of cation in spinel lattices. These results reduce the number of possible defect models. In the following the observed site preference is briefly reviewed.

A recent Mössbauer spectroscopy study by Daniels and Rosencweig[7] has shown that magnetite has an inverse spinel type crystal structure and Fe^{2+} and V_C has a B-site preference at room temperature. On the other hand, Takeuchi and Furukawa[8] suggested that Fe^{2+} is randomly distributed on A- and B-sites at high temperatures. Flood and Hill[9] also assumed a random distribution of Fe^{2+} ions. Dieckmann and Schmalzried[10] have recently analysed the nonstoichiometric data of magnetite based on their tracer diffusion data of Fe and concluded that Fe^{2+} is randomly distributed over A- and B-sites. Although a definite conclusion was not given on the site preference of cation vacancies, they have pointed out that the random distribution of cation vacancies is the most reasonable one to presume.

Trivalent aluminum ions have relatively strong B-site preference, as shown by the normal spinel structure of $FeAl_2O_4$. From his neutron diffraction study and magnetic susceptibility measurements on $FeAl_2O_4$, Roth[11] stated that the structure of $FeAl_2O_4$ can be expressed as $Fe_{0.923}Al_{0.077}(Fe_{0.077}Al_{1.923})O_4$.

Navrotsky and Kleppa[12] reviewed site preference in spinel lattice and evaluated the enthalpy change associated with the reaction:

$$Fe_A^{2+} + Al_B^{3+} \rightleftarrows Fe_B^{2+} + Al_A^{3+}$$

as 9.2 kcal mol^{-1}. They also evaluated the site preference energy of various kinds of cations in the spinel lattice and concluded that Al^{3+} ions have the strongest B-site preference among Fe^{2+}, Fe^{3+}, and Al^{3+} ions.

In summarizing the above investigations, it is concluded that Fe^{2+} and Al^{3+} ions and vacancies prefer B-sites at low temperatures and both ions and vacancy are likely to be distributed randomly at high temperatures. Thus, the twenty seven defect models are reduced to eight defect models. Table 1 shows the description of these eight defect models and the expressions of concentrations of Fe^{2+}, Fe^{3+}, Al^{3+} ions and vacancies V_C on A- and B-sites in terms of moles per mole of $(Fe_{1-y}Al_y)_{3-\delta}O_4$. Notations R and B designate the random distribution and the B-site preference, respectively. Details of the assignment of the concentration are given in Appendix A.

Equilibrium Constants. To determine which one of the eight models listed in Table 1 best interprets the observed nonstoichiometric data, we employed two methods of calculation, the quasi-chemical model (Q.C. model) and the band electron model (B.E. model).

Calculation by the Q.C. Model: In this model Fe^{2+}, Fe^{3+}, and Al^{3+} ions and vacancies are assumed to form an ideal solution in the cation sublattice.

TABLE 1. DESCRIPTION OF POSSIBLE MODELS AND CONCENTRATIONS OF CATIONS AND VACANCIES

Model No.	Distribution of cations[a]			C_i^j		
	Fe^{2+}	V_C	Al^{3+}	Fe_A^{2+}	Fe_A^{3+}	V_A
1	R	R	R	$\frac{1-3\delta}{3}$	$\frac{2(1+\delta)-y(3-\delta)}{3}$	$\frac{\delta}{3}$
2	R	R	B	$\frac{1-3\delta}{3(1-y)}$	$\frac{2(1+\delta)-y(3-\delta)}{3(1-y)}$	$\frac{\delta}{3}$
3	R	B	R	$\frac{1-3\delta}{3-\delta}$	$\frac{2(1+\delta)-y(3-\delta)}{3-\delta}$	0
4	R	B	B	$\frac{1-3\delta}{(1-y)(3-\delta)}$	$\frac{2(1+\delta)-y(3-\delta)}{(1-y)(3-\delta)}$	0
5	B	R	R	0	$\frac{(3-\delta)[2(1+\delta)-y(3-\delta)]}{6(1+\delta)}$	$\frac{\delta}{3}$
6	B	R	B	0	$\frac{3-\delta}{3}$	$\frac{\delta}{3}$
7	B	B	R	0	$\frac{2(1+\delta)-y(3-\delta)}{2(1+\delta)}$	0
8	B	B	B	0	1	0

Model No.	C_i^j				
	Al_A^{3+}	Fe_B^{2+}	Fe_B^{3+}	V_B	Al_B^{3+}
1	$\frac{y(3-\delta)}{3}$	$\frac{2(1-3\delta)}{3}$	$\frac{2[2(1+\delta)-y(3-\delta)]}{3}$	$\frac{2\delta}{3}$	$\frac{2(3-\delta)y}{3}$
2	0	$\frac{(2-3y)(1-3\delta)}{3(1-y)}$	$\frac{(2-3y)[2(1+\delta)-y(3-\delta)]}{3(1-y)}$	$\frac{2\delta}{3}$	$y(3-\delta)$
3	y	$\frac{(2-\delta)(1-3\delta)}{3-\delta}$	$\frac{(2-\delta)[2(1+\delta)-y(3-\delta)]}{(3-\delta)}$	δ	$y(2-\delta)$
4	0	$\frac{[2-\delta-y(3-\delta)](1-3\delta)}{(1-y)(3-\delta)}$	$\frac{[2-\delta-y(3-\delta)][2(1+\delta)-y(3-\delta)]}{(1-y)(3-\delta)}$	δ	$y(3-\delta)$
5	$\frac{y(3-\delta)^2}{6(1+\delta)}$	$1-3\delta$	$\frac{(3+7\delta)[2(1+\delta)-y(3-\delta)]}{6(1+\delta)}$	$\frac{2\delta}{3}$	$\frac{y(3-\delta)(3+7\delta)}{6(1+\delta)}$
6	0	$1-3\delta$	$\frac{3+7\delta-3y(3-\delta)}{3}$	$\frac{2\delta}{3}$	$y(3-\delta)$
7	$\frac{y(3-\delta)}{2(1+\delta)}$	$1-3\delta$	$\frac{(1+2\delta)[2(1+\delta)-y(3-\delta)]}{2(1+\delta)}$	δ	$\frac{y(3-\delta)(1+2\delta)}{2(1+\delta)}$
8	0	$1-3\delta$	$1+2\delta-y(3-\delta)$	δ	$y(3-\delta)$

a) R designates random distribution and B designates localization on B-sites.

The chemical potential of the oxygen equilibrated with the oxide can be obtained by the following equation:

$$\frac{1}{2}(\mu_{O_2}^{\circ}+kT\ln P_{O_2}) = \frac{\partial G(N_1, N_2, N_3, N_4, N_5)}{\partial N_5}, \quad (3)$$

where N_i's with subscripts 1, 2, 3, 4, and 5 are numbers of Fe^{2+}, Fe^{3+}, V_C, Al^{3+}, and O^{2-} in the crystal, respectively, and G is the Gibbs energy of the crystal. The number of sites to be occupied by vacancies is given by the equation

$$N_3 = \frac{3}{4}N_5 - (N_1+N_2+N_4) \equiv \frac{3}{4}(N_5-N_5^{\circ}), \quad (4)$$

where N_5° is the number of oxide ions at the stoichiometric composition. If cations and vacancies form an ideal solution, the Gibbs energy is expressed as follows:

$$G = \frac{N_5^{\circ}}{4}G^{\circ}(N_3=0) + N_3 g_V - TS_{config}, \quad (5)$$

where g_V is the Gibbs energy of forming a cation vacancy, G° is the Gibbs energy of the crystal when $\delta=0$. S_{config} is expressed by

$$S_{config} = k\ln W_A W_B = k\ln \frac{(N_5/4)}{N_1^A!N_2^A!N_3^A!N_4^A!}\frac{(N_5/2)}{N_1^B!N_2^B!N_3^B!N_4^B!}, \quad (6)$$

where superscripts A and B designate A- and B-sites.

Substituting Eqs. 4, 5, and 6 into Eq. 3, the following expression is obtained by a standard calculation:

$$\frac{1}{2}(\mu_{O_2}^{\circ}+kT\ln P_{O_2}) = \frac{3}{4}g_V - kT\sum_{i=1}^{4}\left[\left(\frac{\partial N_i^A}{\partial N_5}\right)\ln\left(\frac{4N_i^A}{N_5}\right) - \left(\frac{\partial N_i^B}{\partial N_5}\right)\ln\left(\frac{2N_i^B}{N_5}\right)\right]. \quad (7)$$

If we express the concentration, the number of moles in one of $(Fe_{1-y}Al_y)_{3-\delta}O_4$, by the notation C_i^j, using a meaning similar to N_i^j, C_i^j can be related to N_i^j and N_5 as follows:

$$C_i^j = 4N_i^j/N_5 \quad (j=A, B;\ i=1, 2, 3, 4). \quad (8)$$

The differentials $(\partial N_i^j/\partial N_5)$ can be expressed by C_i^j

and as follows:

$$\left(\frac{\partial N_i^{\,j}}{\partial N_5}\right) = \frac{1}{4}\left(\frac{\partial C_i^{\,j} N_5}{\partial N_5}\right) = \frac{1}{4}\left(C_i^{\,j} + N_5\frac{\partial C_i^{\,j}}{\partial N_5}\right)$$
$$= \frac{1}{4}\left(C_i^{\,j} + \frac{3}{4}N_5\frac{\partial C_i^{\,j}}{\partial N_3}\right)$$
$$= \frac{1}{4}\left(C_i^{\,j} + 3N_5\frac{N_5^\circ}{N_5^{\,2}}\frac{\partial C_i^{\,j}}{\partial \delta}\right)$$
$$= \frac{1}{4}\left[C_i^{\,j} + \frac{3\left(N_5 - \frac{4}{3}N_3\right)}{N_5}\left(\frac{\partial C_i^{\,j}}{\partial \delta}\right)\right]$$
$$= \frac{1}{4}\left[C_i^{\,j} + (3-\delta)\left(\frac{\partial C_i^{\,j}}{\partial \delta}\right)\right]. \quad (9)$$

In the above calculations the following relations are used, besides Eqs. 4 and 8:

$$\delta = \frac{4N_3}{N_5} = \frac{4N_3}{N_5^\circ + \frac{4}{3}N_3},$$

$$\mathrm{d}\delta = \frac{4N_5^\circ}{N_5^{\,2}}\mathrm{d}N_3.$$

Substituting Eqs. 8 and 9 into Eq. 7, we obtain the following expression:

$$\frac{1}{2}(\mu_{O_2}^\circ + kT\ln P_{O_2}) = \frac{3}{4}g_V - kT\sum_{i=1}^{4}\left[\left(C_i^{\,A} + (3-\delta)\frac{\partial C_i^{\,A}}{\partial \delta}\right)\right.$$
$$\left.\times \ln C_i^{\,A} + \left(C_i^{\,B} + (3-\delta)\frac{\partial C_i^{\,B}}{\partial \delta}\right)\ln (C_i^{\,B}/2)\right].$$

Putting

$$\nu_i^{\,j} \equiv \left(\frac{\partial N_i^{\,j}}{\partial N_5}\right) = \frac{1}{4}\left[C_i^{\,j} + (3-\delta)\frac{\partial C_i^{\,j}}{\partial \delta}\right] \quad (10)$$
$$i = 1, 2, 3, 4;\ \mathrm{j} = \mathrm{A}, \mathrm{B},$$

we obtain

$$\prod_{i=1}^{4}(C_i^{\,A})^{-\nu_i^{\,A}}\prod_{i=1}^{4}(C_i^{\,B}/2)^{-\nu_i^{\,B}}P_{O_2}^{-1/2} = \exp\left[\left(\frac{1}{2}\mu_{O_2}^\circ - \frac{3}{4}g_V\right)\Big/kT\right].$$
$$\equiv K(\mathrm{QC}) \quad (11)$$

Equation 11 is the mass action law for the following defect equilibrium:

$$\nu_1^{\,A}Fe_A^{2+} + \nu_2^{\,A}Fe_A^{3+} + \nu_3^{\,A}V_A + \nu_4^{\,A}Al_A^{3+} + \nu_1^{\,B}Fe_B^{2+}$$
$$+ \nu_2^{\,B}Fe_B^{3+} + \nu_3^{\,B}V_B + \nu_4^{\,B}Al^{3+} + \frac{1}{2}O_2(g) = 0. \quad (12)$$

By using the expressions for $C_i^{\,j}$ in Table 1, the stoichiometric coefficient $\nu_i^{\,j}$ is calculated by Eq. 10. The results are given in Table 2. Details are given in Appendix B. Let us term the defect models described by Eq. 12 as QC-1, QC-2, ···, QC-8 models.

Thus the defect equilibrium equations and the mass action laws can be written explicitly. For example, the equilibrium for model QC-3 is

$$\frac{1}{4}\frac{7+3\delta}{3-\delta}Fe_A^{2+} + \frac{17-11\delta}{4(3-\delta)}Fe_B^{2+} + \frac{y}{4}Al_B^{3+} + \frac{1}{2}O_2(g)$$
$$\rightleftarrows \left[\frac{5+\delta}{2(3-\delta)} - \frac{y}{2}\right]Fe_A^{3+} + \left[\frac{7-5\delta}{2(3-\delta)} + \frac{y}{2}\right]Fe_B^{3+}$$
$$+ \frac{3}{4}V_B + \frac{y}{4}Al_A^{3+} + O_L^{2-}.$$

In this equation the stoichiometric coefficients depend on δ. When equilibrium constants are calculated using Eq. 11 and the expressions of concentration listed in Table 1, δ is canceled in the powers of concentrations and simple expressions are obtained. For example, the equilibrium constant for model QC-3 can be expressed as

$$K(\mathrm{QC\text{-}3}) = \left(\frac{2}{2-\delta}\right)^{1/4}\left(\frac{2+2\delta-(3-\delta)y}{1-3\delta}\right)^{2}\left(\frac{\delta}{2}\right)^{3/4}P_{O_2}^{-1/2}$$

Thus equilibrium constants are easily calculated using observed values of δ and P_{O_2}.

Equilibrium Constants Calculated by the B. E. Model: In the band electron model, Fe^{2+} ions on B-sites are regarded as electron donors in a 3-d band. This is a consequence of the observation that the electric conduction in magnetite and spinel ferrites is caused by the electron movements in a narrow 3-d band formed by Fe ions on B-sites.[13]

TABLE 2. STOICHIOMETRIC COEFFICIENTS FOR VARIOUS MODELS

Model No.	$-\nu_i^{\,j}$							
	Fe_A^{2+}	Fe_A^{3+}	V_A	Al_A^{3+}	$-Fe_B^{2+}$	Fe_B^{3+}	V_B	Al_B^{3+}
1	$\frac{2}{3}$	$-\frac{2}{3}$	$-\frac{1}{2}$	0	$\frac{4}{3}$	$-\frac{4}{3}$	$-\frac{1}{2}$	0
2	$\frac{2}{3(1-y)}$	$-\frac{2}{3(1-y)}$	$-\frac{1}{4}$	0	$\frac{2(2-3y)}{3(1-y)}$	$-\frac{2(2-3y)}{3(1-y)}$	$-\frac{1}{2}$	0
3	$\frac{7+3\delta}{4(3-\delta)}$	$-\frac{2(5+\delta)-2y(3-\delta)}{4(3-\delta)}$	0	$-\frac{y}{4}$	$\frac{17-11\delta}{4(3-\delta)}$	$-\frac{2(7-5\delta)+2y(3-\delta)}{4(3-\delta)}$	$-\frac{3}{4}$	$\frac{y}{4}$
4	$\frac{7+3\delta}{4(1-y)(3-\delta)}$	$-\frac{2(5+\delta)-2y(3-\delta)}{4(1-y)(3-\delta)}$	0	0	$\frac{17-11\delta-8y(3-\delta)}{4(1-y)(3-\delta)}$	$-\frac{2(7-5\delta)+2y(3-\delta)}{4(1-y)(3-\delta)}$	$-\frac{3}{4}$	0
5	0	$-\frac{y(3-\delta)^2}{24(1+\delta)^2}$	$-\frac{1}{4}$	$\frac{y(3-\delta)^2}{24(1+\delta)^2}$	2	$-\left[2-\frac{y(3-\delta)^2}{24(1+\delta)^2}\right]$	$-\frac{1}{2}$	$-\frac{y(3-\delta)^2}{24(1+\delta)^2}$
6	0	0	$-\frac{1}{4}$	0	2	-2	$-\frac{1}{2}$	0
7	0	$-\left[\frac{1}{4}+\frac{y(3-\delta)^2}{32(1+\delta)^2}\right]$	0	$\frac{y(3-\delta)^2}{32(1+\delta)^2}$	2	$-\left[\frac{7}{4}-\frac{y(3-\delta)^2}{32(1+\delta)^2}\right]$	$-\frac{3}{4}$	$-\frac{y(3-\delta)^2}{32(1+\delta)^2}$
8	0	$-\frac{1}{4}$	0	0	2	$-\frac{7}{4}$	$-\frac{3}{4}$	0

Samokhvalov and his co-investigators[14] have measured the electrical conductivity and thermoelectric power of solid solutions of the zinc ferrite-magnetite and nickel ferritemagnetite systems and derived the following expression for the chemical potential of an electron on a B-site:

$$\mu_{e_B^-} = E_C - kT\ln\frac{1}{2}\left[\frac{N_O}{N_D} - 1 + \sqrt{\left(1-\frac{N_O}{N_D}\right)^2 + 4\left(\frac{N_O}{N_D}\right)\exp(E_D/kT)}\right], \quad (13)$$

where E_D is the difference in energy level between the bottom of the conduction band and the donor level, and N_O and N_D are the densities of state of the conduction band and the donor level, respectively. In the present system, N_O and N_D are given as follows:

$$N_O = [Fe_B^{2+}] + [Fe_B^{3+}],$$
$$N_D = [F_Be^{2+}].$$

At high temperatures, the second term in the square root in Eq. 13 can be eliminated and Eq. 13 can be reduced to

$$\mu_{e_B^-} = E_C + kT\ln\frac{N_D}{N_O} = E_C + kT\ln\frac{C_1^B}{C_1^B+C_2^B}. \quad (14)$$

As Fe^{2+} is regarded as $e_B^- + Fe_B^{3+}$, the defect equilibrium is expressed by replacing Fe_B^{2+} in Eq. 12 by $e_B^- + Fe_B^{3+}$. Thus,

$$\nu_1^A Fe_A^{2+} + \nu_2^A Fe_A^{3+} + \nu_3^A V_A + \nu_4^A Al_A^{3+} + \nu_1^B e_B^- + (\nu_1^B+\nu_2^B)Fe_B^{3+} + \nu_3^B V_B + \nu_4^B Al_B^{3+} + \frac{1}{2}O_2 = 0. \quad (15)$$

The mass action law for Eq. 15 is

$$K(BE) = \prod_{i=1}^{4}(C_i^A)^{-\nu_i^A}\prod_{i=1}^{4}(C_i^B/2)^{-\nu_i^B}\left(\frac{C_2^B}{C_1^B+C_2^B}\right)^{-\nu_1^B} = K(QC)\left(\frac{C_2^B}{C_1^B+C_2^B}\right)^{-\nu_1^B}. \quad (16)$$

Fundamental aspects of Eqs. 15 and 16 are described in Appendix B. Let us term the defect models described by Eq. 16 as BE-1, BE-2, ···, and BE-8 models.†

The defect equilibrium equation and mass action law for model BE-3 are, for example,

$$\frac{7+3\delta}{4(3-\delta)}Fe_A^{2+} + \frac{17-11\delta}{4(3-\delta)}e_B^- + \frac{1}{4}(1-2y)Fe_B^{3+} + \frac{y}{4}Al_B^{3+} + \frac{1}{2}O_2 \rightleftarrows \frac{5+\delta}{2(3-\delta)}Fe_A^{3+} + \frac{y}{4}Al_A^{3+} + \frac{3}{4}V_B + O_L^{2-}$$

and

$$K(BE\text{-}3) = \left(\frac{2}{2-\delta}\right)^{1/4}\left(\frac{2+2\delta-y(3-\delta)}{1-3\delta}\right)^2\left(\frac{\delta}{2}\right)^{3/4} \times\left[\frac{2(1+\delta)-y(3-\delta)}{(3-\delta)(1-y)}\right]^{17-11\delta/4(3-\delta)}P_{O_2}^{-1/2}.$$

In this way equilibrium constants for each respective model can be easily calculated by using Eq. 16, using the expressions of ν_i^j and C_i^j in Tables 1 and 2, and the experimental values of δ and P_{O_2}.

† There may arise a question about applying Eq. 14 to models 5—8, where $C_2^B \leq C_1^B$. As no observation has been reported as to the characteristics of an electron band on B-sites if $[Fe_B^{3+}] \lesssim [Fe_B^{2+}]$, Eq. 14 was provisionally assumed to work for models 5—8.

Discussion

Criteria for the Selection of the "best" Model. In order to select the best one of these sixteen defect models, some criteria are necessary. Usually the slope of the log δ *vs.* log P_{O_2} plot is used for the selection. However, the slopes are 2/3 at small values of δ for several models, and also vary with δ. Thus this simple criterion is inadequate for the present purpose. Since the equilibrium constant K should be constant if the model is appropriate, the criteria that the dependence of ln$K$ on δ, as well as the dependence of ln$K$ on y, should be smallest for the "best" model were adopted for the selection. The advantage of this criteria is that one can easily detect the differences among the defect models.

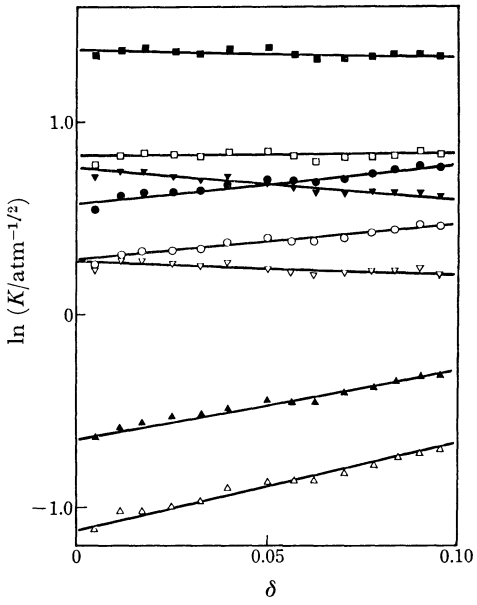

Fig. 3. Values of ln$K$ for respective defect model of $Fe_{3-\delta}O_4$.
○: QC-1, ●: QC-3, △: QC-5, ▲: QC-7, □: BE-1, ■: BE-3, ▽: BE-5, ▼: BE-7.

Analysis of Nonstoichiometric Deta. The equilibrium constants for equilibria 1 to 8 were calculated using Eqs. 11 and 16 and the observed values of δ and P_{O_2}. Figure 3 illustrates the dependence of ln$K$ on δ for $Fe_{3-\delta}O_4$ at 1400 °C. As $y=0$ for magnetite, only the eight equilibrium constants given in this figure were calculated. As is easily seen, ln$K$ changes almost linearly with δ for all the models. The equilibrium constants changed similarly with δ for solid solutions with aluminum ferrite. Thus the relationship between ln$K$ and δ can approximately be represented by the equation

$$\ln K = \alpha\delta + \beta. \quad (17)$$

The value α gives the slope of the ln$K$-δ plot and, according to the critetia adopted above, the model with the samllest absolute value of α is the "best" one.

Figure 4 illustrates the values of α for $(Fe_{0.75}Al_{0.25})_{3-\delta}$-

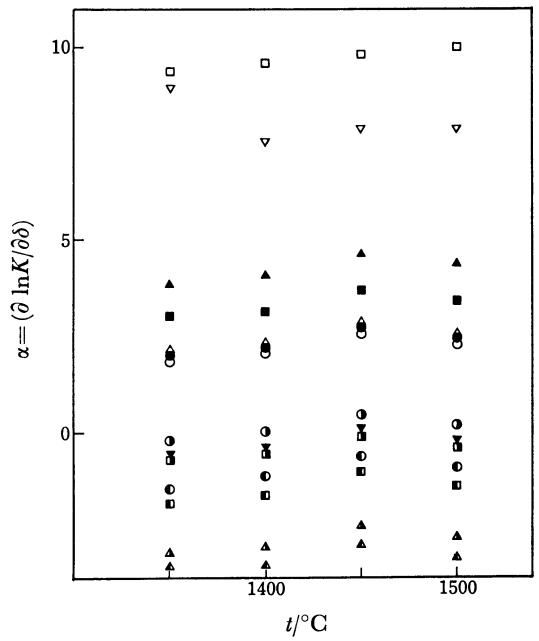

Fig. 4. Values of α for respective defect model of $(Fe_{0.75}Al_{0.25})_{3-\delta}O_4$.
○: QC-1, ●: QC-3, △: QC-4, ▲: QC-5, □: QC-6, ■: QC-7, ▽: QC-8 ▼: BE-1, ◑: BE-2, ◐: BE-3, ◨: BE-5 ◧: BE-6, ◭: BE-7, ◬: BE-8.

O_4. Those for model QC-2 are not given because K(QC-2) has the same value as K(QC-1). Those for model BE-4 are also excluded, since their absolute values are too large. As is easily seen in this figure, the value for QC-1 was the smallest among the QC models, although the differences from those for the QC-3 and QC-4 models. are small. A Similar conclusion has been reached by Dieckmann and Schmalzried[10] in their analysis of the tracer diffusion and nonstoichiometry of magnetite.

The α values for the BE-1 and BE-2 models are very small. They are smaller then those for the QC-1 model and it is concluded that the "best" model would be either the BE-1 or the BE-2 model. But it is difficult to choose the better one of the two only from this figure. A similar calculation was made for $Fe_{3-\delta}O_4$ and $(Fe_{0.67}Al_{0.33})_{3-\delta}O_4$. Figure 5 shows the values of α for K(BE-1)

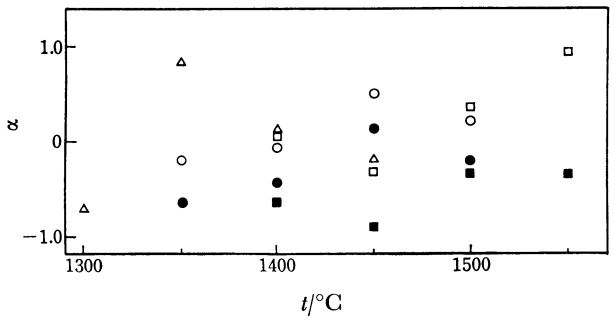

Fig. 5. Values of α for BE-1 and BE-2 models. The open and the solid marks denote the values for BE-1 and BE-2 models, respectively.
△ and ▲: $Fe_{3-\delta}O_4$, ○ and ●: $(Fe_{0.75}Al_{0.25})_{3-\delta}O_4$, □ and ■: $(Fe_{0.67}Al_{0.33})_{3-\delta}O_4$.

and K(BE-2). As is seen from Table 2, values of ν_i^j are the same for models 1 and 2 if $y=0$: Thus the values of α of the BE-1 and BE-2 models are the same for $Fe_{3-\delta}O_4$.

Except for some cases (1500 °C for $y=0.25$, and 1500 and 1550 °C for $y=0.33$), the absolute values of α are smaller for the BE-2 model than for the BE-1 model. This preference for the BE-2 model is also supported by the dependence of $\ln K$ on y. Figure 6 shows the plot of $\ln K$ against y. Clearly equilibrium constants for the BE-2 model depend less on y than those for the BE-1 model. The result indicates that the BE-2 model is better than the BE-1 model and, therefore, the BE-2 model was chosen as the "best" model in this investigation.

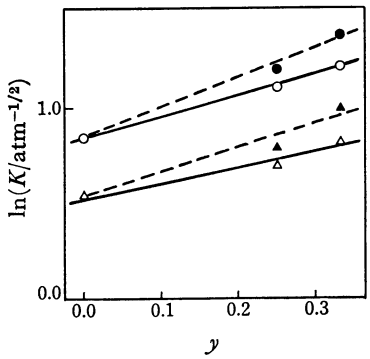

Fig. 6. Dependence of $\ln K$ on y.
●: 1400 °C, BE-1 model, ○: 1400 °C, BE-2 model, ▲: 1450 °C, BE-1 model, △: 1450 °C, BE-2 model.

BE-2 Model and Equilibrium Constant. The BE-2 model which has been chosen as the "best" model can be characterized as follows:
(1) Fe^{2+}, Fe^{3+} ions, and vacancies distribute randomly on A- and B-sites.
(2) Al^{3+} ions are localized on B-sites.
(3) Fe^{2+} and Fe^{3+} ions on B-sites provide a narrow d-band whose Fermi level can be approximated by Eq. 14.
The explicit expression of the defect equilibrium and

Table 3. Values of $\ln K$(BE-2)

T/°C	$\ln(K/\text{atm}^{-1/2})$		
	$y=0$	$y=0.25$	$y=0.33$
1300	1.767± 0.007		
1350	1.219± 0.002	1.493± 0.006	
1400	0.833± 0.01	1.11± 0.01	1.231± 0.002
1450	0.547± 0.003	0.709± 0.01	0.843± 0.008
1500		0.305± 0.0002	0.463± 0.007
1550			0.110± 0.004
$\Delta H°$/kcal mol^{-1}	−43.7± 3.6	−45.3± 1.3	−45.7± 0.9
$\Delta S°$/cal K^{-1} mol^{-1}	−24.4± 2.2	−24.9± 0.8	−24.9± 0.5

Figures after ± signs are standard deviations.

the equilibrium constant are given as follows:

$$\frac{2}{3(1-y)}Fe_A^{2+} + \frac{2(2-3y)}{3(1-y)}e_B^- + \frac{1}{2}O_2(g) \rightleftarrows \frac{2}{3(1-y)}Fe_A^{3+} + \frac{1}{4}V_A + \frac{1}{2}V_B + O_L^{2-}, \quad (18)$$

$$K(\text{BE-2}) = \left[\frac{(3-\delta)(1-y)}{1-3\delta}\right]^{2(2-3y)/3(1-y)} \times \left[\frac{2+2\delta-y(3-\delta)}{1-3\delta}\right]^{2/3(1-y)} \left(\frac{\delta}{3}\right)^{3/4} P_{O_2}^{-1/3}. \quad (19)$$

Table 3 gives the values of $\ln K(\text{BE-2})$ together with values of ΔH° and ΔS° for Reaction 18. It is noteworthy that ΔH° and ΔS° are negative and almost independent of y.

The large negative values of ΔS° would be due to the disappearance of $O_2(g)$ and e_B^- in Reaction 18. The large negative value of ΔH° comes mainly from the negative partial molar enthalpy of oxygen in magnetite and its solid solutions with $FeAl_2O_4$.

Appendix

A. Assignment of Concentration of Ions and Vacancy. The concentrations of ions and vacancies for respective model are given in Table 1 in terms of moles in one mole of $(Fe_{1-y}Al_y)_{3-\delta}O_4$. One mole of $(Fe_{1-y}Al_y)_{3-\delta}O_4$ has 1 and 2 mol of A- and B-sites, respectively. Over these 3 mol of cation sites, $1-\delta$, $[2(1+\delta)-y(3-\delta)]$, $y(3-\delta)$, and δ mol of Fe^{2+}, Fe^{3+}, Al^{3+} ions, and vacancies, respectively, are distributed.

To elucidate the concentrations on the A- and B-sites the following procedure was adopted.

1) First, the concentration of vacancies was assigned. In the case of random distribution vacancies were assumed to be distributed in the ratio of 1:2 over A and B sites. If the vacancy is localized on a B-site, the concentration of the B-site is δ and that on the A-site is 0.

2) Concentrations of localized Fe^{2+} and/or Al^{3+} ions are assigned in the second step. When they are localized on a B-site, the concentrations on the B-site are $1-3\delta$ and $y(3-\delta)$ for Fe^{2+} and Al^{3+} ions, respectively. Concentrations on an A-site are 0 when they are localized on a B-site.

3) Concentrations of randomly distributed Fe^{2+} and/or Al^{3+} ions are determined in the third step. In this calculation, it was assumed that the concentration on A- or B-site is proportional to the number of sites still remaining at this step. For example, in model 5 the concentrations of Fe^{2+} and V_C are already assigned and the numbers of remaining sites are $1-\delta/3$ and $(3+7\delta)/3$ for A- and B-sites, respectively. Thus the concentration of Al^{3+} on A-site is calculated as

$$y(3-\delta) \times \frac{(1-\delta/3)}{(1-\delta/3)+(3+7\delta)/3} = \frac{y(3-\delta)^2}{6(1+\delta)}.$$

4) Finally the concentration of Fe^{3+} ion is assigned by allotting them on the remaining cationic sites.

B. Stiochiometric Coefficients and Equilibrium Conditions.

Equation 11 implies that a mass action law holds between the defects in the crystal of $(Fe_{1-y}Al_y)_{3-\delta}O_4$. The stoichiometric coefficients can be calculated by using Eq. 10. An illustration is given below for model 2.

The expressions for stoichimetric coefficients, ν_i^j's are calculated by using the expressions in Table 1 for C_i^j's. For example, ν_1^A is calculated as follows:

$$\nu_1^A = \frac{1}{4}\left[C_1^A + (3-\delta)\frac{\partial C_1^A}{\partial \delta}\right] = \left[\frac{1-3\delta}{3(1-y)} + (3-\delta)\frac{-3}{3(1-y)}\right]\Big/4 = -2/3(1-y).$$

Other coefficients are calculated in the same way; the results are given in Table 2. Using these values of ν_i^j's, Eq. 11 is written as follows:

$$(C_1^A)^{-2/3(1-y)}\cdot(C_2^A)^{2/3(1-y)}\cdot(C_3^A)^{1/4}\cdot(C_1^B/2)^{-2(2-3y)/3(1-y)} \times (C_2^B/2)^{2(2-3y)/3(1-y)}\cdot(C_3^B/2)^{1/2}\cdot P_{O_2}^{-1/2} = \frac{[V_A]^{1/4}[Fe_A^{3+}]^{2/3(1-y)}([V_B]/2)^{1/2}([Fe_B^{3+}]/2)^{2(2-3y)/3(1-y)}}{[Fe_A^{2+}]^{2/3(1-y)}([Fe_B^{2+}]/2)^{2(2-3y)/3(1-y)}P_{O_2}^{1/2}} = \exp\left[\frac{1}{2}\left(\mu_{O_2}^\circ - \frac{3}{4}g_V\right)\Big/kT\right]. \quad (A\text{-}1)$$

Equation A-1 implies that the defect equilibrium for this model can be described by the following chemical equilibrium:

$$\frac{2}{3(1-y)}Fe_A^{2+} + \frac{2(2-3y)}{3(1-y)}Fe_B^{2+} + \frac{1}{2}O_2 \rightleftarrows \frac{2}{3(1-y)}Fe_A^{3+} + \frac{2(2-3y)}{3(1-y)}Fe_B^{3+} + \frac{1}{4}V_A + \frac{1}{2}V_B. \quad (A\text{-}2)$$

The equilibrium condition for Eq. A-2 can also be expressed in terms of chemical potential of defects as follows:

$$\frac{2}{3(1-y)}\mu(Fe_A^{3+}) + \frac{2(2-3y)}{3(1-y)}\mu(Fe_B^{3+}) + \frac{1}{4}\mu(V_A) + \frac{1}{2}\mu(V_B) - \frac{2}{3(1-y)}\mu(Fe_A^{2+}) - \frac{2(2-3y)}{3(1-y)}\mu(Fe_B^{2+}) - \frac{1}{2}\mu_{O_2} = 0. \quad (A\text{-}3)$$

Thus the general expression of the defect equilibria, Eq. 11, implies the equilibrium condition in terms of the chemical potential, μ_i^j, of the i-th ion on the j site.

$$\frac{1}{2}\mu_{O_2} + \sum_{\substack{j=A,B \\ i=1,2,3,4}} \nu_i^j \mu_i^j = 0. \quad (A\text{-}4)$$

The conduction electrons in the BE models are considered to be created by the ionization of Fe_B^{2+} ions and the following virtual equilibrium is conceived.

$$Fe_B^{2+} \rightleftarrows Fe_B^{3+} + e_B^-. \quad (A\text{-}5)$$

For this equilibrium the following expression holds for the chemical potential of Fe_B^{2+} ions:

$$\mu(Fe_B^{2+}) = \mu(Fe_B^{3+}) + \mu_{e_B^-}. \quad (A\text{-}6)$$

Incorporating Eq. A-6 into A-4, an equilibrium conditions for BE modles is obtained:

$$\frac{1}{2}\mu_{O_2} + \nu_{Fe^{2+}}^A\mu(Fe_A^{2+}) + \nu_{Fe^{3+}}^A\mu(Fe_A^{3+}) + \nu_{V_C}^A\mu(V_A) + \nu_{Al^{3+}}^A\mu(Al_A^{3+}) + \nu_{Fe^{2+}}^B[\mu(Fe_B^{3+}) + \mu_{e_B^-}] + \nu_{Fe^{3+}}^B\mu(Fe_B^{3+}) + \nu_{V_C}^B\mu(V_B) + \nu_{Al^{3+}}^B\mu(Al_B^{3+}) = 0. \quad (A\text{-}7)$$

Equation A-7 implies the mass action law, Eq. 16, and the equilibrium equation, Eq. 15, for defect equilibrium, when BE models are adopted.

References

1) L. S. Darken and R. W. Gurry, *J. Am. Chem. Soc.*, **68**, 798 (1946).
2) O. N. Salmon, *J. Phys. Chem.*, **65**, 550 (1961).
3) J. Smiltens, *J. Am. Chem. Soc.*, **79**, 4877, 4881 (1957).

4) B. D. Roiter, *J. Am. Ceram. Soc.*, **47**, 509 (1964).
5) A. Nakamura, S. Yamauchi, K. Fueki, and T. Mukaibo, *J. Phys. Chem. Solids*, **39**, 1203 (1978).
6) R. C. Evans, "An Introduction to Crystal Chemistry," 2nd ed, Cambridge Univ. Press (1964), p. 174.
7) J. M. Daniels and A. Rosencweig, *J. Phys. Chem. Solids*, **30**, 1561 (1969).
8) S. Takeuchi and K. Furukawa, *Sci. Repts. Res. Inst. Tohoku Unive., Ser. A*, **12**, 120 (1960).
9) H. Flood and D. G. Hill, *Z. Elektrochem.*, **61**, 18 (1957).
10) R. Dieckmann and H. Schmalzried, *Ber. Bunsenges. Phys. Chem.*, **81**, 414 (1977).
11) W. W. Roth, *J. Phys.*, **5**, 507 (1964).
12) A. Navrotsky and O. J. Kleppa, *J. Inorg. Nucl. Chem*, **29**, 2701 (1967).
13) C. F. Jefferson and C. K. Barker, *IEEE Trans. Magn.* **4**, 460 (1968).
14) A. A. Samokhvalov and A. G. Rustamov, *Soviet Phys. Solid State*, **7**, 961 (1965).